Supplementary Information

KEGG pathway sign test

KEGG pathway release 92.0 was downloaded using KEGGREST R package. We used the sign test to test for independent *cis* changes showing deviations from neutralality, thus pointing to lineage-specific selection[9,49]. If any pathway deviates significantly from the random expectation, then the null hypothesis of neutrality can be rejected in favor of polygenic selection. We discarded pseudogenes and used pathways with a minimum of 50 genes linked to them, with no threshold on ASE significance. *Drug metabolism - other enzymes*, *Steroid hormone biosynthesis*, *Drug metabolism - cytochrome P450,* and *Metabolism of xenobiotics by cytochrome P450* pathways were removed from the analysis as genes associated with them are found mainly in clusters and therefore their expression changes cannot be treated as independent events. Disease and genetic information processing pathways (e.g., *Transcription*) were not tested. Chromosome 20 and chromosome X were removed from the analyses as well due to potential aneuploidy[12] and non-random deactivation that could shift results. We also examined how various FDR and fold-change thresholds affect the test and found that the down:up ratio among Hh genes increases as more stringent thresholds are used (Extended Data Fig. 3a).

Similarly, we tested protein translation rates[52]. This dataset provided information for 34 out of the 50 Hh proteins annotated in KEGG. Differential translation rates data (33 of the proteins) and detectable/non-detectable translation levels data (one protein) were combined for the sign test analysis.

EVC2 expression

To pick a top candidate for further analyses, we took all genes that are expressed in both hybrid cell types (mean FPKM >= 1), show significant ASE in both, and are linked to at least one HPO phenotype with human-chimpanzee divergence information (see above). Out of 268 such genes, EVC2 was the gene farthest from the origin of axes (Fig. 3b). For its phenotypic analyses, phenotypes were extracted from HPO build 1268 and from a review of the literature (Supplementary Tables 21-23).

EVC2 acts in a complex with EVC, whose loss-of-function phenotypes are indistinguishable from EVC2. We detect up-regulation of *EVC* human alleles compared to chimpanzees in the hybrid CNCCs (2.25x, FDR = 2.52×10^{-19}), but not parental samples, suggesting counteracting *cis*- and *trans*-acting changes. As the abundance of the EVC/EVC2 complex is determined by the less abundant protein[91], and the expression levels of *EVC* are 7-8x higher than those of *EVC2* in parental and hybrid CNCCs, it is likely that the down-regulation of EVC2 reduces the overall abundance of the complex.

DPSCs

Human DPSCs: Human DPSCs were ordered from Lonza (catalog #PT-5025). Cells were grown in DPSC medium catalog #: PT-3005 (AXOL).

Chimpanzee DPSCs: An incisor and a canine tooth were recovered from a forty-seven year old female chimpanzee euthanized for clinical reasons at the Yerkes National Primate Research Center. The teeth surfaces were cleaned and dissected at the cementum-enamel junction to reveal

the pulp chamber. The dental pulp was recovered followed by digestion in 3 mg/ml collagenase type I (Invitrogen, Inc.) and 4 mg/ml of dispase (Invitrogen, Inc) for one hour at 37°C. The cell suspension was filtered through a 70 μm cell strainer (Falcon, Inc) to remove cell debris and undigested tissues. The single-cell suspensions of the dental pulp were recovered and cultured in α-MEM (Invitrogen, Inc.) media supplemented with 20% fetal bovine serum (Hyclone, Inc), 100 μm L-ascorbic acid-2-phosphate (Sigma, Inc), 2 mM glutamine, 100 units/ml penicillin and 100 μg /ml streptomycin (Invitrogen, Inc.), and incubated at 37°C with 5% CO_2. Medium was replaced every three to four days and cells were passaged at 80% confluence. Cells were grown in DPSC medium catalog #: PT-3005 (AXOL).

Candidate regions underlying EVC2 differential expression

CNCC ATAC-seq, and NR2F1 and TFAP2A ChIP-seq reads were downloaded from GEO accession number GSE70751. Reads were aligned to the human hg38 and chimpanzee panTro5 genomes using Bowtie2 [92] and the parameters --very-sensitive –dovetail --maxins 2000. Peaks were called using MACS2 v2.1.1.20160309 [93] with the parameters -g hs -B -q 0.05. First, we searched for any region within the gene body or promoter (up to 5 kb upstream) of *EVC2* for loci with an ATAC-seq peak in all individuals of one species, but none of the individuals of the other species (two chimpanzees and three humans, with two replicates each, except for human 1). Three such loci were found (hereinafter, intron 6, intron 9 and intron 19, Extended Data Fig. 4a-c). Next, we picked the boundaries for the sequences used for the reporter assay (see next) based on the center of TFAP2A or NR2F1 binding (the stronger of the two transcription factors per each locus), up to 10 kb away from the ATAC-seq peak. Given its regulatory role, the promoter of *EVC2* was cloned as well. We also cloned a locus within intron 1 which was previously

reported to bear chimpanzee-biased H3K27ac marks[43] (but did now show any species-specific chromatin accessibility).

To construct reporter plasmids containing chimpanzee and human *EVC2* genomic loci, DNA sequences were amplified from genomic DNA samples using primers listed in Supplementary Table 24. The amplified products were then inserted into the pGL4.11b (Promega) vector for the promoter and pGL4.23 (Promega) vector for candidate enhancers. Cloned DNA sequences were validated by Sanger sequencing. For the chimpanzee sequence within intron 6, we were unable to amplify the full region denoted by the primers from genomic DNA due to repetitive regions. Instead, we were able to amplify a 626 bp sequence that included the beginning and end of the region, without the repeats in its center (Supplementary Table 25). We confirmed that the sequence was still specific to *EVC2* intron 6 via the UCSC Genome Browser BLAT tool. This 626 bp is in fact more homologous to the human sequence than the entire length, as the repeats in the center of the chimpanzee sequence do not exist in the human sequence. For the intron 19 locus, repetitive sequences in the primer regions did not allow us to clone sequences with identical boundaries: the resulting chimpanzee sequence had additional 16 bp in its 5' end, and 45 bp in its 3' end, while the rest of the 1.4 kb was homologous. Reporter plasmids and the Renilla luciferase plasmid pGL4.73 (Promega) were co-transfected into human DPSCs in each well of a 48-well plate using X-tremeGENE HP DNA Transfection Reagent (Sigma-Aldrich) according to the manufacturers' protocol. To correct for transfection efficiency, 240 ng of reporter plasmid and 60 ng of pGL4.73 were transfected. 48 hours post-transfection, cells were harvested and reporter activity was measured using the Dual-luciferase reporter assay system (Promega) according to the manufacturers' protocol. Reporter activity was quantified using the

Glomax 96-well plate luminometer (Promega). Relative firefly/Renilla luciferase values were determined in two independent experiments of quadruplet measurements (n = 8).

The intron 6 and 19 loci showed increased expression of the chimpanzee allele (3.6-fold and $P = 8.2\text{x}10^{-4}$ for intron 6, and 4.1-fold and $P = 9.4\text{x}10^{-4}$ for intron 19, one-tailed *t*-test, Extended Data Fig. 4d,e). The promoter and intron 9 loci did not show significant differential expression ($P = 0.07$ for the promoter, and $P = 0.08$ for intron 9, one-tailed *t*-test), while the intron 1 locus showed human-biased expression ($P = 4.7\text{x}10^{-9}$). Based on the ATAC-seq data, intron 1 is not accessible in either species. Therefore, it remains to be determined whether this region plays an active regulatory role *in vivo* (possibly attenuating the effect of other loci), or alternatively, has the potential to drive differential expression, but is not accessible in its endogenous context. The intron 6 and intron 19 loci each have over ten substitutions between humans and chimpanzees, making the investigation of specific expression-altering sequence changes a challenging task. The intron 19 locus also has two indels (7 bp and 24 bp long), and the intron 6 locus has a 1.2 kb long indel. Given its length, the 1.2 kb indel serves as a promising candidate to underlie the expression difference we observed. Comparing this locus with the gorilla genome (gorGor5), we found that this sequence does not exist in gorillas, suggesting that the insertion likely emerged along the chimpanzee lineage. At first glance, this does not fit with the observed differential expression of *EVC2*, which likely emerged along the human lineage. However, although humans show lower *EVC2* expression compared to gorillas (Extended Data Fig. 3e), the human-gorilla ratio is lower than the human-chimpanzee ratio, suggesting there might have been an additional event along the chimpanzee lineage increasing *EVC2* expression. Importantly, the chimpanzee region amplified for the reporter assay did not include most of this insertion (due to its repetitiveness), and therefore serves as a more closely matched sequence to the human sequence.

Regardless, the comparative ATAC-seq, TFAP2A and NR2F1 analyses described above identified sites outside this insertion showing chimpanzee-biased patterns. This suggests that intron 6 might have experienced a more complex regulatory evolution, with changes affecting *EVC2* expression in both directions.

To identify potential sequence changes that might underlie these expression changes, we scanned the intron 6 and intron 19 loci for predicted transcription factor binding sites that differ between human and chimpanzees. We downloaded the 4,351 *directly determined* human transcription factor binding motifs from the Catalogue of Inferred Sequence Binding Preferences (CIS-BP) database (http://cisbp.ccbr.utoronto.ca/), and used FIMO[94] to map each motif to the human and chimpanzee sequences. For each predicted binding site, we required that at least one species had a binding q-value ≤ 0.05. Then, we searched for instances where the predicted binding score of the motif differed between the species. In the intron 6 locus, we found 1,091 predicted binding differences, all of which are in the repetitive regions of the intron, and 51 of those are within the homologous repetitive region that is outside the chimpanzee insertion. In the intron 19 locus, we found 31 predicted binding differences, and two additional predicted binding motifs outside the region that was amplified in the human sequence (Supplementary Tables 26-27). Next, we analyzed ChIP-seq data from ENCODE[95] to determine if any of the predicted binding sites are indeed bound by the predicted transcription factor in embryonic stem cells (as CNCC ChIP-seq data for these factors were not available). We found that four of the transcription factors (TCF12, RXRA, SP1, and SRF) were mapped in the ENCODE project. For one of them (SRF) there are reported peaks (chr4:5573026-5573222 and chr4:5573079-5573309) overlapping the predicted motif in intron 19 (chr4:5573215-5573228). SRF is expressed in CNCCs (TPM = 39.2), suggesting this binding site may be occupied by this factor in CNCCs as well. Notably, none of

the positions of the substitutions in intron 6 nor intron 19 are particularly conserved among vertebrates (PhyloP score range: -3.54 to -0.13 for intron 6, and -3.42 to 0.07 for intron 19). Thus, further work is required to determine whether the expression changes we report were driven by these divergent sequences, and if so, to tease out the individual contribution of each of these substitutions and indels to the overall expression change.

Supplementary Table 24: Genomic coordinates, primers and vectors used in the construction of chimpanzee (Ch) and human (Hu) *EVC2* reporter plasmids.

Reporter Plasmid	Genomic Coordinates	Genomic DNA Primers	pGL vector
EVC2 promoter	panTro5=chr4:6171370-6174138	Fwd: CCAGCTTGTTTCTAGTTTGTT TCATCATTTCCTCATGGC Rev: TGGGCCAGACCATTGACC	pGL4.11b
	hg38=chr4:5707417-5710191	Fwd: CCAGCTTGTTTCTAGTTTGTTTCATCATTTC CTCATGGC Rev: TGGGCCAGACCATTGGCC	pGL4.11b
EVC2 intron 1	panTro5=chr4:6164402-6166648	Fwd: GCAGACCATTCTACTGGAAGTTG Rev: AAATACACCCATGTGGTCTCTGA	pGL4.23
	hg38=chr4:5700284-5702536	Fwd: GCAGACCATTCTACTGGAAGTTG Rev: CTTAACAAATACATCCATGTGGTC	pGL4.23
EVC2 intron 6	panTro5=chr4:6146850-6148511	Fwd: CAGAAACTCTGAATGAAATGAAATG Rev: GGGGTTCCTAAGGGGTAGAG	pGL4.23
	hg38=chr4:5683604-5684029	Fwd: CAGAAACTCTGAATGAAATGAAATG Rev: GGGGTTCCTAAGGGGTAGAG	pGL4.23
EVC2 intron 9	panTro5=chr4:6106169-6107052	Fwd: GATCAGTGGGGTGGCTATC Rev: TTGATCAACTGCGGTCTTTATTC	pGL4.23
	hg38=chr4:5647354-5648240	Fwd: GATCAGTGGGGTGGCTATC Rev: TTGATCAACTGCGGTCTTTATTC	pGL4.23

EVC2 intron 19	panTro5=chr4:6031719-6033215	Fwd: AGAGGATGCTCAATCAGTGCTAA Rev: ATAACAGGCATGGCAGGTGTT	pGL4.23
	hg38=chr4:5573074-5574468	Fwd: CCAGTCGATGTCTTTTCTGTGAT Rev: GTGTTCAGGAAGTACCAGCTCCT	pGL4.23

Supplementary Table 25: Chimpanzee *EVC2* intron 6 locus amplified from genomic DNA sample.

GGGGTTCCTAAGGGGTAGAGTCAATATCACAGACAGGAACCAAACAAAGTAACAGGCGGGACTAT
TTCAGGGTGGGGCAGGGGAAGCCACGAGGAAGGTCCTCCCGGAGCATGCAGGGAGCCAGGCTCTG
CGGAACCACAAACCTCCCCCTGCTCAAGCCAGCCCAGCCCAGGAACACACACAGCTGCCCAGGAAC
ACACACAGCTGGCCAGGAACACACACAGCTGCCCAGGAACACACACAGCTGCCCGGGAACATACA
CACAGCTGCCCGGGAACACACACAGCTGCCCGGGAACACACACAGCTGCCCGGGAACACACACAC
AGCTGCCCGGGAACACACACAGCTGCCCGGGAATACGCACAGCTGCCCGGAAACACACACAGCTG
CCCAGGAACACACACAGCTGCCCAGGAACACACAGAGCTGCCCGGGAACATACACACAGCTGCCC
GGGAACACACACAGCTGCCCAGGAACACACACAGCTGCCCAGGAACACACAGAGCTGCCCGGGAA
CACACACAGCTGCCCGGGAACACACACAGCTGCCCGGGGCTTCAGCTCCTGAGGCTCCTGCCTGAG
GACATGGAAGCTTCCATTTCATTTCATTCAGAGTTTCTG

See Supplementary Figure for BLAST[96] alignments.

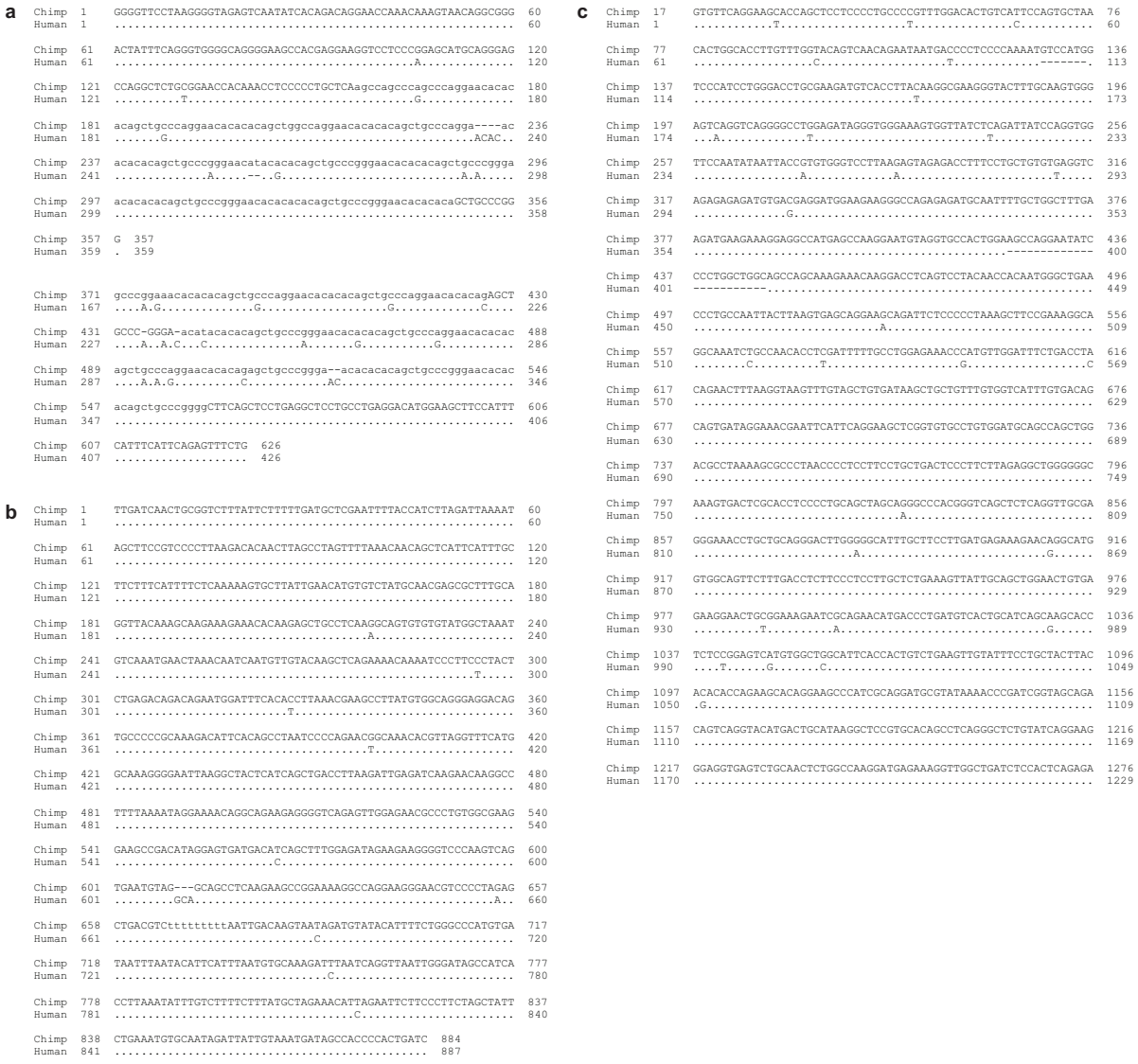

Supplementary Figure. BLAST alignment between the chimpanzee and human amplified sequences for intron 6 (a), 9 (b) and 19 (c). Dots represent identities, lowercase letters show low complexity sequences.

We also used the CNCC ATAC-seq data to map peaks in putative enhancers associated with Hh genes. To do so, we downloaded the GeneHancer database[97] (v4_12) and extracted the 530 putative enhancers associated with Hh genes. For each putative enhancer, we investigated chimpanzee and human ATAC-seq peaks 10 kb around it (Supplementary Table 28).

EVC2 effect on hedgehog signaling output

Stable cell line generation

Evc2$^{-/-}$ NIH/3T3 Flp-In cells were generated using CRISPR/Cas9 genome editing using the guide sequence 5'-gatatttcaaaaatgctcac-3', and were described previously in Pusapati et al.[91]. Doxycycline-inducible Evc2 expression was generated by cloning mouse Evc2 (N-terminally tagged with 3xHA (downstream of signal sequence) and C-terminally tagged with 1D4) into the pCDH-Lenti-TRE-rtta3G-BLAST plasmid (gifted from Atul Kumar). Lenti-virus was generated by transfection of this construct in combination with psPAX2 (Addgene plasmid number 12260) and pVSVG (Addgene plasmid number 14888) into 293T cells. Lenti-viral supernatant was then added to *Evc2*$^{-/-}$ NIH/3T3 Flp-In cells for 48 hours before selection with puromycin (Calbiochem).

Generation of pooled cell lines expressing low, medium and high amounts of mouse Evc2 was carried out by cloning mouse Evc2 C-terminally tagged with TEV-YFP-FLAG into the pMSCV plasmid (Addgene plasmid number 24828). The pMSCV construct was then transfected into Bosc23 helper cells in order to generate retroviral supernatants[98]. Virus was added to *Evc2*$^{-/-}$ NIH/3T3 Flp-In cells after 24 and 48 hours by centrifugation for 1 hour at 800g. Stably infected cells were then selected by puromycin. High multiplicity of infection was evident by the death of only a small fraction (~5%) of cells. These cells were sorted into pools of 100,000 cells each by fluorescence activated cell sorting in order to isolate low, medium and high expressing pooled lines.

Cell culture and Hedgehog signaling assays

Both *Evc2*$^{-/-}$ NIH/3T3 Flp-In cells and Dental Pulp Stem Cells (DPSCs) were grown in high glucose Dulbecco's Modified Eagle's Medium (DMEM) (Thermo Fisher Scientific) containing 10% Fetal Bovine Serum (FBS) (Sigma), 2 mM L-glutamine (Gemini Biosciences), 1× MEM nonessential amino acids solution (Gibco), penicillin (40 U/ml) and streptomycin (40 μg/ml) (Gemini Biosciences), and 1 mM sodium pyruvate (Gibco).

In order to test for Sonic Hedgehog ligand responsiveness, cells were ciliated by growing to confluency and then exchanging the media to low serum (0.5% FBS) DMEM containing the aforementioned supplements for either 24 hours (NIH/3T3 Flp-In cells) or 48 hours (DPSCs). Sonic Hedgehog ligand (recombinant protein generated as in Bishop et al.[99]) and doxycycline (Sigma, D9891) were added 24 hours prior to cell lysis and Western Blotting.

Primary antibodies used for Western Blotting include: mouse monoclonal anti-GLI1 (Cell Signaling, Cat# 2643; RRID: AB_2294746), mouse monoclonal anti-alpha tubulin (clone DM1A, Sigma-Aldrich, Cat#T6199; RRID: AB_477583), rabbit polyclonal anti-P38 (Abcam, Cat# ab7952; RRID: AB_306166), rabbit anti-GFP (Novus Biologicals, NB600-308), rabbit polyclonal anti-SUFU (produced in rabbits (Josman Laboratories) and affinity purified before use), rabbit polyclonal anti-EVC2 (produced in rabbits (Cocalico Biologicals) and affinity purified before use). Secondary antibodies used for Western Blotting include: Peroxidase AffiniPure Donkey Anti-Mouse IgG (H+L) (Jackson ImmunoResearch Laboratories, Cat#715-035-150; RRID:AB_2340770), Peroxidase AffiniPure Donkey Anti-Rabbit IgG (H+L) (Jackson ImmunoResearch Laboratories, Cat#111-035-144; RRID: AB_2307391) and Peroxidase AffiniPure Donkey Anti-Goat IgG (H+L) (Jackson ImmunoResearch Laboratories, Cat#705-035-003; RRID: AB_2340390).

EVC2 CNCC-specific KO mice

All mice were maintained and used in compliance with the Institutional Animal Care and Use Committee (IACUC) of the University of Michigan in accordance with the National Institutes of Health guidelines for Care and Use of animals in research, and all experimental procedures were approved by the IACUC of the University of Michigan. All mice were housed in ventilated cages with free access to food and water. Ventilated cages were in rooms in 18-23 C with 40-60% humidity. Housing room has a 12 hours dark/light cycle with light starting from 6 am.

Two loxP sites were inserted to intron 12 and 14 of the *Evc2* locus, respectively. Cre-dependent recombination caused truncation at exon 15 to generate no functional protein[63]. Neural crest-specific *Evc2* mutant mice were generated by crossing *Evc2* floxed mice with *Wnt1-Cre* mice[100]. Animals were harvested at postnatal day 28 (P28) for structural analyses.

Micro-CT scanning of fixed skulls was taken at the University of Michigan using a micro-CT system (mCT100 Scanco Medical, Bassersdorf, Switzerland). Scan settings were as following: voxel size 12 mm, 55 kVp, 109 mA, 0.5 mm AL filter, and integration time 500 ms. Heterozygous mice were used as controls because they are phenotypically indistinguishable from wildtype mice[63].

To quantify skull morphological differences between controls and *Evc2* KO P28 mice, surface models were first generated based on micro-CT data. Next, each Ellis-van Creveld craniofacial phenotype was examined between control and KO mice and compared to phenotypes that separate humans and chimpanzees, as described above and in Gokhman et al[48]. For the *increased forehead height* phenotype, we examined frontal bone height. *Tapering of the lower face* was equated to ventral rotation of the lower face and micrognathia.

DICOM files/images obtained from micro-CT were used to generate 3D model using ITK-SNAP (www.itksnap.org). 3D slicer (www.slicer.org) was then used for placements of anatomical landmarks. The mandible associated measurements were determined using landmarks from Extended Data Fig. 6c, i.e., mandible length (1-4), condyle head width (3-4), gonial angle (the angle of 5-7 and 4-8) and mandible height (2-6). The thickness of the palate bone was determined at the palate bone at first molar levels. The root length and enamel thickness were determined in molar 1 of controls and KOs. Width of the nasal bone was determined at the most anterior part of nasal bones. These data were combined with previous measurements from *Evc2* KO mice, including of soft tissues[63,64,68].

Supplementary Figure. BLAST alignment between the chimpanzee and human amplified sequences for intron 6 (a), 9 (b) and 19 (c). Dots represent identities, lowercase letters show low complexity sequences.

Supplementary Information References

91. Pusapati, G. V. *et al.* CRISPR Screens Uncover Genes that Regulate Target Cell Sensitivity to the Morphogen Sonic Hedgehog. *Dev. Cell* (2018). doi:10.1016/j.devcel.2017.12.003

92. Langmead, B. & Salzberg, S. L. Fast gapped-read alignment with Bowtie 2. *Nat. Methods* (2012). doi:10.1038/nmeth.1923

93. Zhang, Y. *et al.* Model-based analysis of ChIP-Seq (MACS). *Genome Biol.* (2008). doi:10.1186/gb-2008-9-9-r137

94. Grant, C. E., Bailey, T. L. & Noble, W. S. FIMO: Scanning for occurrences of a given motif. *Bioinformatics* (2011). doi:10.1093/bioinformatics/btr064

95. Bernstein, B. E. *et al.* An integrated encyclopedia of DNA elements in the human genome. *Nature* **489**, 57–74 (2012).

96. Altschul, S. F., Gish, W., Miller, W., Myers, E. W. & Lipman, D. J. Basic local alignment search tool. *J. Mol. Biol.* (1990). doi:10.1016/S0022-2836(05)80360-2

97. Fishilevich, S. *et al.* GeneHancer: genome-wide integration of enhancers and target genes in GeneCards. *Database (Oxford).* (2017). doi:10.1093/database/bax028

98. Pear, W. S., Nolan, G. P., Scott, M. L. & Baltimore, D. Production of high-titer helper-free retroviruses by transient transfection. *Proc. Natl. Acad. Sci. U. S. A.* (1993). doi:10.1073/pnas.90.18.8392

99. Bishop, B. *et al.* Structural insights into hedgehog ligand sequestration by the human hedgehog-interacting protein HHIP. *Nat. Struct. Mol. Biol.* (2009). doi:10.1038/nsmb.1607

100. Danielian, P. S., Muccino, D., Rowitch, D. H., Michael, S. K. & McMahon, A. P. Modification of gene activity in mouse embryos in utero by a tamoxifen-inducible form of Cre recombinase. *Curr. Biol.* (1998). doi:10.1016/s0960-9822(07)00562-3

262